

A comparison of exact, approximate, and linearized ray tracing methods in transversely isotropic media

Patrick F. Daley, Edward S. Krebs, and Laurence R. Lines

ABSTRACT

The exact eikonals for the quasi-compressional (qP) and quasi-shear (qS_V) modes of seismic wave propagation in a transversely isotropic (TI) medium are considered. These are compared in a travel time sense with *weak* anisotropic and *linearized* approximations. The comparisons involve ray propagation in a $2D$ plane layered structure where the axis of anisotropy need not necessarily be aligned with the local coordinate system. The motivation for this is to determine the accuracy of the approximate and linearized eikonals when compared to the exact eikonal for the computation of ray paths in a media displaying weak anisotropy. This exercise is an initial step in addressing an analogous but more complex problem, specifically, ray tracing in orthorhombic media. This $3D$ symmetry is becoming more fundamental in seismic data processing and modeling as $3D$ seismic acquisition methods become the norm rather than the exception. As a consequence, the development of relevant software for processing and modeling of the more complex media types should be available in a variety of forms.

A single rotation angle is used here, about the x_2 spatial axis, or equivalently the p_2 axis in slowness space, as ray propagation is assumed to be $2D$, in the (x_1, x_3) Cartesian plane. For higher order rotations in $3D$ media, it is convenient to consider the more general $2D$ problem as a subset of orthorhombic symmetry, which is being dealt with in ongoing works. To minimize the complexity of this discussion, the anisotropic parameters are assumed to be homogeneous within a layer. This is done to obtain an accurate comparison of travel time results using exact, approximate, and linearized methods.

INTRODUCTION

In the geophysical literature, exact wave propagation in anisotropic media, specifically quasi-compressional (qP) and quasi-shear (qS_V) waves in a medium displaying transversely isotropic (TI) symmetry, has been treated in numerous works, most of which are referenced in the text of Cerveny (2001). A recent paper by Tang and Li (2008) contains a comprehensive list of recent citations related to ray propagation in TI media. To avoid duplication, interested readers are referred to these works. Other relevant and complex solution methods to the general ray tracing problem may be found in the works of Zhou and Greenhalgh (2004), finite element methods; Iversen (2001), perturbation methods; and Iversen and Pšenčík (2008), dynamic ray tracing theory.

The transversely isotropic model used in this paper is the same as that described by Tsvankin (2001). Velocities in the (x_1, x_2) plane are rotationally invariant about the vertical x_3 axis. As indicated by Tsvankin (2001), TI models have a single axis of rotational symmetry, and these models are considered appropriate for sedimentary layered systems containing shale formations (which comprise about 75% of the clastic fill of sedimentary basins. Consequently, the TI

model is a widely used anisotropic model in exploration seismology as the elastic properties can be described by five elastic constants.

Approximations to the exact eikonal for both qP and qS_V wave propagation modes may also be found in a variety of publications, but for the purposes of this work the paper of Gassmann (1964) is fundamental. A more recent description of the qP and qS_V propagation modes may be found in Shearer (1999). The linearization technique, employed to derive the fundamental approximate expressions for the most general quasi – compressional, qP problem was initially presented in Backus (1965) and more recently in Pšenčík and Farra (2005) where it is referred to as First Order Ray Tracing (FORT). The quasi – shear case, qS_V for a TI medium in two dimensions follows from those derivations. A subsequent publication, Farra and Pšenčík (2008), deals with the shear wave modes in a general anisotropic medium type. In the $2D$ transversely isotropic symmetry being considered here, the qS_V case may be written in an analytic form. For higher order anisotropic symmetries, such as the orthorhombic problem (Schoenberg and Helbig, 1996), this is not possible as the two shear modes in that problem are coupled, leading to a more complex situation (Farra and Pšenčík, 2008).

Some of the statements above regarding exact and approximate theories may appear contradictory. In a transversely isotropic medium, the coupled $qP - qS_V$ modes of propagation have their polarization vectors confined to the plane of incidence, while the polarization vector of the independently propagating qS_H mode is normal to this plane. As a consequence of the linearization of the general anisotropic problem, the result is that, in at least the first order approximation, the qP mode propagates independently, and the two shear modes are coupled in $3D$ Cartesian space. This may appear to be inconsistent with the TI situation discussed above. In the case of an orthorhombic medium (Schoenberg and Helbig, 1996) where the exact eikonals are the numerical solutions of a cubic equation, and the roots (eikonals) are arranged in increasing order of magnitude. In symmetry planes this degenerates. The discrepancy mentioned above is a result of this in a $2D$ TI medium. A more detailed discussion of this is beyond the scope of this work.

The ray tracing method used in this work follows the standard formulation for this problem type where the vector components of ray velocity are obtained from an eikonal equation or equivalently, the related Hamiltonian, using well known partial differential equation solution methods. The rays or characteristics specify the paths along which energy is propagated. Generalization of the methods described here to more complex (specifically, $3D$) anisotropic symmetries using the FORT (linearized) formulation is fairly straightforward, and any additional complexity introduced results from considering $3D$ rather than $2D$ structures.

It is required to determine an analogue of Snell's Law at a plane interface between two TI media. This will be treated in what follows for a transversely isotropic medium. It should be noted that for the $2D$ case of the problem considered here quantities related to the solution of the Snell's Law problem may be obtained graphically, at least to some minimal precision.

Before proceeding further, a mathematically informal explanation of the duality of the ray or group velocity space and slowness space should be indicated. For a point on the ray (group

velocity) surface, the vector starting at the origin of this surface, say a point source, and normal to the tangent plane at the point at which the ray touches the ray surface is equal in direction to the corresponding vector in slowness space, and its magnitude in slowness space is equal to the inverse of its magnitude in ray space. The dual of this is that in slowness space, for some arbitrary slowness vector, the vector beginning at the origin of the slowness surface that is normal to the tangent plane at the point at which the slowness vector contacts the slowness surface, is equal in direction to the corresponding ray vector and has a magnitude that is the inverse of the length of the vector in slowness space. This is shown schematically in Figures 1-4. More formal discussions of the above statements may be found in works on differential geometry such as do Carmo (1976).

The use of a plane layered medium may appear overly simplistic. However, the extension of what is presented to more complex geological structures follows as anisotropic axes not aligned with the model axes is similar in a computational nature to models with dipping interfaces. The further step to “blocky type” 2D geological structures is not that much more of an endeavour. More comprehensive techniques are required when ray tracing in a general 3D anisotropic medium with arbitrarily varying symmetry axes and complex geological structure.

THEORETICAL BACKGROUND

The eikonal, $G_m(p_i, x_j)$ or, equivalently, the characteristic equation, for the m^{th} wave propagation mode, is a nonlinear partial differential equation, and is closely related to the Hamiltonian of the system. In a general anisotropic medium the three modes of wave propagation are, $m = qP, qS_1$ or qS_2 ; a quasi – compressional (qP), and two quasi – shear (qS_1 and qS_2). Solutions of each of these eikonal equations, which are quasi – linear partial differential equations (Gassmann, 1964), describe the characteristics or rays of the corresponding wave type propagation. In what follows, only the coupled qP and qS_V modes will be considered. The equations of the vector components of the characteristics or rays of these partial differential equations may be written in terms of Cartesian spatial (x_i) and Cartesian slowness (p_j) coordinates as (Courant and Hilbert, 1962, Červený, 2001)

$$\frac{dx_i}{dt} = \frac{1}{2} \frac{\partial G_m(x_i, p_i)}{\partial p_i}, \quad \frac{dp_i}{dt} = -\frac{1}{2} \frac{\partial G_m(x_i, p_i)}{\partial x_i} \quad (1)$$

This system of first order simultaneous differential equations is the foundation for an initial value problem where t is time and the problem is fully specified by the conditions

$$\mathbf{x}_0 = \mathbf{x}(t_0) \quad , \quad \mathbf{p}_0 = \mathbf{p}(t_0) \quad (2)$$

for some initial time t_0 . It is to be remembered that energy propagation occurs along the rays or characteristics. In a 2D symmetry plane in a TI medium, the $qP(+)$ and $qS_V(-)$ are coupled and will be considered here, however, the qS_H problem will not as in the symmetry being used, it propagates independently of the other two modes with an elliptic ray surface.

Exact Eikonals:

The first case considered are the exact eikonals given by the equations

$$G_{qP/qS_V}(x_i, p_i) = \frac{1}{2} \left[(A_{11} + A_{55}) p_1^2 + (A_{33} + A_{55}) p_3^2 \pm \left[A_\alpha + A_\alpha (1 + 4\sigma_D)^{1/2} - 1 \right] \right] = 1 \quad (3)$$

where quantities in the above requiring definition are the slowness vector components, p_j

$$p_j = \frac{n_j}{v_{qP/qS_V}(n_j)} \quad \mathbf{p} = (p_1, p_3) \quad \mathbf{n} = (n_1, n_3) \quad (4)$$

The expressions $v_{qP/qS_V}(n_j)$ are the phase or wavefront normal velocities. These are obtained from the eikonal equations by substituting the definitions of p_1 and p_3 in terms of n_j and $v_{qP/qS_V}(n_j)$ into equation (3).

Given a wavefront propagating in a *TI* medium, described by the phase function, $\tau(x_i)$, the wavefront normal (phase) vector, \mathbf{n} , is defined as

$$\mathbf{n} = \frac{\nabla \tau}{|\nabla \tau|} = (\sin \theta, \cos \theta) \quad (5)$$

so that

$$\mathbf{p} = \nabla \tau = \left(\frac{\sin \theta}{v(\theta)}, \frac{\cos \theta}{v(\theta)} \right) \quad (6)$$

As mentioned above, expressions for the phase velocity $v_{qP/qS_V}(n_j)$ result from substituting (6) into equation (3). Equations (3) – (6) are valid (when used in context) for all three of the possible eikonal type specifications: exact, approximate, and linearized. The other required necessary definitions are

$$A_\alpha = (A_{11} - A_{55}) p_1^2 + (A_{33} - A_{55}) p_3^2 \quad (7)$$

$$\sigma_D = \frac{A_D p_1^2 p_3^2}{A_\alpha^2} \quad (8)$$

with

$$A_D = (A_{13} + A_{55})^2 - (A_{11} - A_{55})(A_{33} - A_{55}). \quad (9)$$

From equations (1) and (3), the ray (group) vector components for qP (+) and qS_V (-) propagation modes may be obtained in the form

$$\frac{dx_1}{dt} = \frac{p_1}{2} \left\{ (A_{11} + A_{55}) \pm \frac{1}{A_\alpha [1 + \sigma_D]^{1/2}} \left[A_\alpha (A_{11} - A_{55}) + 2A_D p_3^2 \right] \right\} \quad (10)$$

$$\frac{dx_3}{dt} = \frac{p_3}{2} \left\{ (A_{33} + A_{55}) \pm \frac{1}{A_\alpha [1 + \sigma_D]^{1/2}} \left[A_\alpha (A_{33} - A_{55}) + 2A_D p_1^2 \right] \right\} \quad (11)$$

and as the *TI* medium has been chosen to be homogeneous

$$\frac{dp_1}{dt} = \frac{dp_3}{dt} = 0 \quad (12)$$

so that $p_j = \text{constant}$ along a specific ray. This holds for all three situations dealt with here.

The ray (group) angle, Θ , is defined with respect to the vertical spatial axis as

$$\tan \Theta = \frac{dx_1/dt}{dx_3/dt}, \quad (13)$$

and the magnitude of the ray (group) velocity is

$$V_g = \left[\left(\frac{dx_1}{dt} \right)^2 + \left(\frac{dx_3}{dt} \right)^2 \right]^{1/2} = \left[\frac{d\mathbf{x}}{dt} \cdot \frac{d\mathbf{x}}{dt} \right]^{1/2}. \quad (14)$$

Approximate Eikonals:

The approximate eikonals are obtained under the assumption that the quantity $|A_D| \ll 1$ (weak anisotropy) in equation (3). A_D is a measure of the deviation of the qP and qS_V wavefronts from the ellipsoid of revolution and the spherical, respectively. The $qP(+)$ and $qS_V(-)$ eikonals in a *TI* medium in this situation have the form (Gassmann, 1964)

$$G_{qP/qS_V}(x_i, p_i) = \frac{1}{2} \left[(A_{11} + A_{55}) p_1^2 + (A_{33} + A_{55}) p_3^2 \pm \left[\frac{2A_D p_1^2 p_3^2}{A_\alpha} + A_\alpha \right] \right] = 1 \quad (15)$$

Following the method described for the exact case in the previous section, the ray (group) vector components for the $qP(+)$ and $qS_V(-)$ modes are given by

$$\frac{dx_1}{dt} = \frac{p_1}{2} \left[(A_{11} + A_{55}) \pm \left[\frac{2A_D (A_{33} - A_{55}) p_3^4}{A_\alpha^2} + (A_{11} - A_{55}) \right] \right] \quad (16)$$

$$\frac{dx_3}{dt} = \frac{p_3}{2} \left[(A_{33} + A_{55}) \pm \left[\frac{2A_D (A_{11} - A_{55}) p_1^4}{A_\alpha^2} + (A_{33} - A_{55}) \right] \right] \quad (17)$$

Linearized Eikonals:

In the third instance, the linearized quasi-compressional $qP(+)$ and quasi-shear $qS_V(-)$ phase velocities in a TI medium may be written as (Backus, 1965, and Pšenčík and Farra, 2005)

$$v_{qP/qS_V}^2(n_j) = \frac{1}{2} \left[(A_{11} + A_{55})n_1^2 + (A_{33} + A_{55})n_3^2 \pm \left[2E_{13}n_1^2n_3^2 + A_\alpha \right] \right] \quad (18)$$

As before

$$\mathbf{n} = (n_1, n_2) = (\sin \theta, \cos \theta) \quad (19)$$

where θ is the polar angle associated with the phase or wavefront normal velocities, $p_j = n_j/v(n_k)$ and E_{13} , the anelliptic term, which is the linearized equivalent of A_D in the previous two cases, is defined as

$$E_{13} = 2(A_{13} + 2A_{55}) - (A_{11} + A_{33}) \quad (20)$$

After some manipulation of the expression for the phase velocities the $qP(+)$ and $qS_V(-)$ linearized eikonals in this case have the forms

$$G_{qP/qS_V}(x_j, p_j) = \frac{1}{2} \left[(A_{11} + A_{55})p_1^2 + (A_{33} + A_{55})p_3^2 \pm \left[2E_{13}p_1^2p_3^2 / (p_k p_k) + A_\alpha \right] \right] = 1 \quad (21)$$

and the $qP(+)$ and $qS_V(-)$ components of the ray (group) velocity vector components are obtained as

$$\frac{dx_1}{dt} = \frac{p_1}{2} \left[(A_{11} + A_{55}) \pm \left[2E_{13}p_3^4 / (p_k p_k)^2 + (A_{11} - A_{55}) \right] \right] \quad (22)$$

$$\frac{dx_3}{dt} = \frac{p_3}{2} \left[(A_{33} + A_{55}) \pm \left[2E_{13}p_1^4 / (p_k p_k)^2 + (A_{33} - A_{55}) \right] \right] \quad (23)$$

where $(p_k p_k) = p_1^2 + p_3^2$.

SNELL'S LAW IN A TI MEDIUM

A derivation of Snell's Law for all three ray propagation methods will be considered in the two following subsections. However, as they are similar, a generic approach is used, with the required formulae for each of the three cases given at the end of the first subsection. Two situations are considered; determination of the reflected and transmitted horizontal components of the slowness vector when both the reflected and transmitted slowness surfaces are unrotated (first subsection) or rotated (second subsection).

Snell's Law for the Non-rotated Case

It will initially be assumed that the axes of anisotropy, in both the incident (upper) and transmitted (lower) layer are aligned with the intervening interface, so that the reflected ray would have the same magnitude and acute angle with the normal at the point of incidence as the incident ray. It is to be remembered that the approximate expressions employed here are for *weakly anellipsoidal* anisotropy and it will be assumed that this constraint will not be seriously violated in what follows. This is shown graphically in Figure (1) where the reflected ray vector is equal in magnitude to the incident ray vector, both vectors making the same acute angle with respect to the normal to the interface as do the corresponding slowness vectors.

If the vector $\mathbf{p} = (p_1, p_3)$ is known, (actually only p_1 in model coordinates is required) the sines of the phase angle in the upper (reflection) and lower (transmission) medium ($x = \sin \theta_r, x = \sin \theta_t$) will be used as the parameters to be determined in terms of a known incident horizontal slowness vector component. For the case of reflection in the upper medium, the incident horizontal slowness vector component is equal to the reflected horizontal slowness vector component so that the acute reflected phase angle in the upper medium measured with respect to the local coordinate system is equal to the incident phase angle.

In the lower medium, the sine of the transmitted phase angle, $\sin \theta_t = x$, is obtained by equating the known incident horizontal slowness vector component with the transmitted horizontal slowness vector component, so that

$$p_1 = \frac{\sin \theta}{v(\theta)} = \frac{x}{v(x)}, \quad x = \sin \theta \quad (24)$$

which is an equation that may also be solved analytically. The solution of the above equation uses the phase, not the group angle. The equations for the phase velocities for the qP and qS_V wave types are given explicitly by equations (18). These quantities for the exact and approximate problems are obtained by substituting (6) into equations (3) and (15). However, once the phase angle is obtained, the components of the transmitted ray vector may be computed using formulae (22) and (23). For the linearized case the solution of the quartic equation (24) (quadratic in x^2) follows from the result of the solution of

$$\begin{aligned} ax^4 + bx^2 + c &= 0 \\ a &= E_{13}p_1^2 \\ b &= -(A_{11}p_1^2 - A_{33}p_1^2 + E_{13}p_1^2 - 1) \\ c &= -A_{33}p_1^2 \end{aligned} \quad (25)$$

The sine of the transmitted qS_V phase angle may be obtained in an analogous manner.

It should be noted here that in all three cases being investigated, for the degenerate ellipsoidal case ($E_{13} = A_D = 0$) the solution of x for the reflected/transmitted qP mode is the same, having the analytic form

$$x = \frac{p_1 \sqrt{A_{33}}}{(1 - (A_{11} - A_{33}) p_1^2)^{1/2}}. \quad (26)$$

In a like manner for the qS_V mode

$$x = p_1 \sqrt{A_{55}}. \quad (27)$$

An alternative approach for obtaining x is to numerically solve an equation of the form

$$F(x) = p_1 v(x) - x = 0. \quad (28)$$

This method of solution is required to be used in the more general case when the anisotropic axes are rotated with respect to the model axes and will be treated in a subsequent section. Also, for more complex symmetries such as a TI medium in a $3D$ structure, which is one of the simplest subsets of the general orthorhombic problem, this method of solution, or some equivalent numerical technique, is required. It should be mentioned that a TI medium has its own intrinsic features that are not limited by the more constrained inherent features fundamental in the orthorhombic subset designation, specifically the coupling of the two shear wave modes.

As was mentioned previously, the determination of x is similar and just minimally more complicated for the approximate and exact cases than for the linearized problem, only the final formulae will be given for the transmitted qP problem. As in the linearized case, the qS_V solution for x follows from the qP problem. The approximate qP eikonal results from the solution for x of

$$\begin{aligned} ax^4 + bx^2 + c &= 0 \\ a &= (B_{13}^2 - A_D) p_1^2 - B_{13} \\ b &= (B_{13} B_{35} + A_{33} B_{13} + A_D) p_1^2 + B_{35} \\ c &= A_{33} B_{35} p_1^2 \end{aligned} \quad (29)$$

where $B_{13} = A_{11} - A_{33}$ and $B_{35} = A_{33} - A_{55}$. The exact formulation for the qP case requires that x be obtained by solving the following equation set,

$$\begin{aligned} ax^4 + bx^2 + c &= 0 \\ a &= (1 - p_1^2 B_{13}) + p_1^4 A_D \\ b &= -(p_1^2 (A_{33} + A_{55}) - p_1^4 A_{55} B_{13} - p_1^4 A_D) \\ c &= p_1^4 A_{33} A_{55} \end{aligned} \quad (30)$$

with $B_{13} = A_{11} - A_{33}$, as before.

Snell's Law for the Rotated Case

The transmitted and reflected slowness vectors, and as a result the rays, generally propagate at different angles in a layer where the axes of anisotropy are rotated by some known angle, ϕ (positive clockwise) with respect to the local axes. It has again been assumed for simplicity that the layers are plane parallel. In the case of curved or dipping interfaces, the condition that the horizontal component of the slowness vector be continuous at the plane boundary is replaced by requiring that the tangential component(s) of the slowness vector at the point of incidence at the arbitrary boundary type be continuous. It should also be reiterated that the measurement of the angles of the transmitted and reflected slowness vectors are taken as the acute angles that they make with the vertical (p_3) axis or in a rotated system with the p'_3 axis. Applying simple trigonometric relations, shown in Figures (2-4), the analogue of Snell's Law in a rotated TI medium is, apart from the introduction of the rotation angle, ϕ , very similar to the unrotated case. Here, $\theta' = \theta + \phi$. The solution method is also similar, but requiring a numerical rather than analytic progression. In terms of the horizontal (tangential) component of the slowness vector in model coordinates, p_1 ,

$$F(\theta, \theta') = p_1 v(\theta') - \sin \theta = 0 \quad [F(x, x') = p_1 v(x') - x = 0] \quad (31)$$

Newton's Method is possibly the best manner of seeking a solution for the above problem. However, if a reasonably accurate guess of the solution can be made, so that it may be bracketed, then Brent's Method (Press et al., 1997) would be a better choice as the derivative of $F(x', x)$ with respect to x or, or equivalently with respect to $\sin \theta$, is not required. In matters such as this, a programmer's previous experience is most often the best indicator of the solution method to be employed.

Specific examples of Snell's Law for reflection and transmission at a plane interface between two TI media are shown in Figures (1) – (4). All schematics employ ellipses – qP (circles – qS_V) rather than more complicated slowness surfaces, for drawing simplicity. The solution methods shown are reasonably accurate from a graphical perspective as quasi – drafting software was used. There were numerous examples which could have been used to present the concept of the analogue of Snell's Law in TI media. However, only four standards were chosen from which other situations may be inferred. Those included here are the qP reflection from an interface due to qP incidence with no rotation of the anisotropic axis in the incident medium (Figure 1), the same type of incidence and reflection from an interface where there is rotation in the incident medium (Figure 2), a qP wave incident and a reflected qS_V wave from an interface where there is rotation in the incident medium (Figure 3), and transmission of a qP wave into a medium where the axis of anisotropy is rotated with respect to the model coordinates (Figure 4). Each figure except (3) is composed of two parts. The first (a) shows the relationship between the incident, reflected or transmitted slowness vector and the related group velocity vector, while the second indicates the method used to obtain relevant angles together with reflected or transmitted slowness (inverse phase velocity) vectors. More specific information is contained in each of the four figure captions.

RAY TRACING METHOD

In a medium composed of N plane parallel transversely isotropic homogeneous layers where the source and receiver are both located at the surface, a description of converted qP and qS_V ray propagation is given by the nonlinear equation

$$G(\Theta_j) = r - \sum_{j=1}^M n_j^{(qP\uparrow)} h_j \tan \Theta_j^{(qP\uparrow)} - \sum_{j=1}^M n_j^{(qP\downarrow)} h_j \tan \Theta_j^{(qP\downarrow)} - \sum_{j=1}^M n_j^{(qS_V\uparrow)} h_j \tan \Theta_j^{(qS_V\uparrow)} - \sum_{j=1}^M n_j^{(qS_V\downarrow)} h_j \tan \Theta_j^{(qS_V\downarrow)} \quad (32)$$

where $G(\Theta_j)$ has been used to indicate $G(\Theta_j) = G(\Theta_j^{(qP\uparrow)}, \Theta_j^{(qP\downarrow)}, \Theta_j^{(qS_V\uparrow)}, \Theta_j^{(qS_V\downarrow)})$. This is a general statement of the problem that allows for rotation of the anisotropic axes in any of the layers. In the above equation, $M (M \leq N)$ is the deepest layer traversed by the ray, h_j - thickness of the j^{th} layer, and r - the horizontal distance between the source and receiver. The number of upward (\uparrow) and downward (\downarrow) propagating qP ray segments in the j^{th} layer are given by $n_j^{(qP\uparrow)}$ and $n_j^{(qP\downarrow)}$. The qS_V cases of ray segment propagation within a layer are similarly indicated. The acute angle that a ray segment makes with the vertical axis in the j^{th} layer, is Θ_j with the superscript on this quantity defining the mode and direction of propagation. At the stationary point, $G(\Theta_j) = 0$. This is the value at which the values of Θ_j produce the minimum travel time between the source and receiver, corresponding to equation (32) satisfying Fermat's principle (Aki and Richards, 1980). The travel time of the general ray described in (32) above, with $V(\Theta_j)$ indicating ray velocity, has the form

$$\tau(\Theta_j) = r - \sum_{j=1}^M \frac{n_j^{(qP\uparrow)} h_j}{\cos \Theta_j^{(qP\uparrow)} V(\Theta_j^{(qP\uparrow)})} - \sum_{j=1}^M \frac{n_j^{(qP\downarrow)} h_j}{\cos \Theta_j^{(qP\downarrow)} V(\Theta_j^{(qP\downarrow)})} - \sum_{j=1}^M \frac{n_j^{(qS_V\uparrow)} h_j}{\cos \Theta_j^{(qS_V\uparrow)} V(\Theta_j^{(qS_V\uparrow)})} - \sum_{j=1}^M \frac{n_j^{(qS_V\downarrow)} h_j}{\cos \Theta_j^{(qS_V\downarrow)} V(\Theta_j^{(qS_V\downarrow)})} \quad (33)$$

where, in a similar manner to the one used in (32), $\tau(\Theta_j)$ is used to denote that $\tau(\Theta_j) = \tau(\Theta_j^{(qP\uparrow)}, \Theta_j^{(qP\downarrow)}, \Theta_j^{(qS_V\uparrow)}, \Theta_j^{(qS_V\downarrow)})$.

In the $2D$ TI ray tracing problem, the right hand side of (32) is specified for this problem indicating that upgoing and downgoing ray segments of the same mode within a layer do not, in general, correspond to an equal displacement in the horizontal direction, that is, there may be a rotation of the anisotropic axes in any or all of the layers. For this reason, the "primes" on Θ_j , the ray angles with a layer have been omitted as they are implied with the introduction of the " \uparrow " and " \downarrow " notation. Thus, a ray composed of any number of ray segments propagating

through the layered medium and travelling a distance r from a surface source to a surface receiver must satisfy $G(\Theta_j) = 0$, which produces the proper ray propagation solution for the specified ray. Both source and receiver have been assumed to be located on the surface with the source located at the origin of a Cartesian system, which is aligned with the plane layered medium, and the vertical axis, x_3 , is chosen to be positive downwards. Upward and downward propagating ray segments of the same mode of propagation within a layer where the axis of anisotropy is not aligned with the plane layered model system generally do not make the same angle with the vertical. It is for this reason that upward and downward propagating ray segments for a propagation mode in an arbitrary layer are considered separately.

Embedded in this generally nonlinear equation is another generally nonlinear equation for the analogue of Snell's Law, formulated in terms of phase velocities and angles, discussed in an earlier section. Thus, this "two - point" ray tracing scheme is at least minimally numerically intensive. As in the Snell's Law section, a choice must be made as to what form of numerical solution is most efficient. Equation (32) may be parameterized in one quantity; ray angle in a given layer, horizontal component of the slowness vector in a given layer, to name but two. As to the method to be used, given that this is a single parameter nonlinear problem, Brent's Method (Press et al., 1997) would be suggested, but as previously stated, a programmer's preference should ultimately be the decisive determinant. Considerations that should be kept in mind are that any code written should be flexible enough to advance to more complex situations, such as dipping layers and some basic forms of inhomogeneity with minimum effort.

NUMERICAL RESULTS

An anisotropic model which could be described as moderately, as opposed to weakly, anisotropic was chosen for the computation of numerical results. This model is a somewhat modified version of an olivine symmetry plane. The anisotropic parameters, A_{ij} , used are given in Table 1, together with other related normalized quantities. The qP and qS_V ray (group) velocity and slowness surfaces are displayed in Figure (5), employing the exact eikonal equations. As travel time differences are what were to be determined, a single plane parallel layer with an anisotropic axis rotation of 15° was used. The slight modifications of the A_{ij} used were done in order to establish, using a split spread shooting geometry, at least the angle at which a ray leaves the source and returns along the same path. Other points of interest, such as the angle at which the ray leaves the source in a manner that the reflected ray at the surface displays normal incidence, were also considered.

The anisotropic layer was chosen to be $5km$ thick, with a qP surface source, and receivers placed at the surface from $-10km$ to $10km$. The two cases considered using exact, approximate, and linearized, formulations were qP rays emanating from the source and being reflected back to the surface as either qP or qS_V rays. From Table 1 it may be seen that the value of σ (dimensionless quantity indicating the deviation of the ray (group) velocity or slowness surfaces from the elliptical) is such that it is clear that the assumptions used to obtain approximate and linearized forms of the eikonal equation have been violated. This was purposely done to ascertain the effects on the two non-exact solutions employed. The results are shown in three panels in each of Figures (6) and (7). The rays are displayed for the surface locations from

$-10km$ to $10km$ at $0.5km$ increments (panel (a)). For the travel time computations the increment was reduced to $0.05km$ for a total of 401 equally spaced points along the surface receiver spread. Only the rays computed using the exact method are displayed. The reference travel time curves were also obtained from the exact formulation (panel (b)). The percentage differences between the exact travel times and those obtained from the approximate and linearized eikonal equations are shown in panel (c) of the two figures. These were calculated as $\%_{DIFF} = [(\tau_{exact} - \tau_{approx./linear}) / \tau_{exact}] \times 100$.

Entering the domain where three arrivals due to the triplication points on the qS_V ray surface could not be avoided. To maintain single valued ray arrivals and travel time curves, the point on the slowness surface which corresponded to the fastest arrival, was taken to be the geometrical arrival at certain points in Figure (7). This area corresponds to that section of the travel time difference plot where the linearized approach deviates most from the exact formula.

For completeness, a comparison of the travel times for the TI and isotropic cases is made in Figure (8). The P and S_V isotropic velocities, α and β , given by $\alpha = \sqrt{A_{33}}$ and $\beta = \sqrt{A_{55}}$. Panel (a) shows the incident P - reflected P case, panel (b) the incident P - reflected S_V case and panel (c) the percentage differences between the TI and isotropic computations. The difference percentages are obtained as previously using $\%_{DIFF} = [(\tau_{aniso.} - \tau_{iso.}) / \tau_{aniso.}] \times 100$.

An older Fujitsu ($1.7GHz$) laptop was used for the computations. Both **g95** and Lahey-Fujitsu **If95** compilers were employed, with nearly identical run times. These run times were of the order of $1.5s$ for the geometry described above, using a receiver spacing of $0.005km$ (4001 rays). In an attempt to emulate computation times for similar problems done three decades ago, an IBM386 was resurrected and the oldest available Lahey **If90** compiler installed. As expected, the run times were significantly greater. With the superior hardware options presently available, and the confidence that these will advance geometrically, if not exponentially, the problem of ray tracing in complex geometrical $3D$ structures for seismic applications such as modeling or migration should be of minimal concern.

CONCLUSIONS

The basic formulae and solution method for tracing rays in a plane layered transversely isotropic homogeneous $2D$ medium have been presented. The rotationally invariant vertical axis of anisotropy need not be aligned with the corresponding model axis. Exact, approximate, and linearized forms of the qP and qS_V eikonals and related phase and group velocities were used in the development. A form of Snell's Law analogous to that used for the isotropic homogeneous problem was presented. Although the exact eikonals were considered, the model used was such that it did violate the constraint of *weak* anisotropy so that the formulae for the approximate and linearized eikonals were marginally used out of context with no excessive deviations from the exact theory. Possibly the most significant feature that is indicated in Figures (6) and (7) is that the linearized formulation deviates less than the approximate formulation from the exact solution. This may be due to the fact that the *weak* anisotropic assumption was violated and the linearized solution adapted better to the situation. This is one of the subjects of an ongoing sensitivity study, which includes inversion methods.

REFERENCES

- Backus, G.E., 1965, Possible forms of seismic anisotropy of the uppermost mantle under oceans, *Journal of Geophysical Research*, 70, 3429-3439.
- Courant, R. and Hilbert, D., 1962, *Methods of Mathematical Physics, Vol. II: Partial Differential Equations*: Interscience Publications, New York.
- Červený, V., 2001, *Seismic Ray Theory*, Cambridge University Press, Cambridge.
- do Carmo, M., 1976, *Differential geometry of curves and surfaces*, Prentice-Hall, New Jersey.
- Farra, V and Pšenčík, I., 2008, First-order ray computations of coupled S waves in inhomogeneous weakly anisotropic media, *Geophysical Journal International*, 173, 979–989.
- Gassmann, F., 1964, Introduction to seismic travel time methods in anisotropic media: *Pure and Applied Geophysics*, 58, 63-112.
- Iversen, E., 2001, First-order perturbation theory for seismic isochrones, *Studia Geophysica et Geodætica*, 45, 395-444.
- Iversen, E. and Pšenčík, I., 2008, Ray tracing and inhomogeneous dynamic ray tracing for anisotropy specified in curvilinear coordinates, *Geophysical Journal International*, 174, 316–330
- Press, W.H., Teukolsky, S.A., Vetterling, W.T. and Flannery, B.P., 1997, *Numerical recipes for Fortran 77*, Press Syndicate, New York, NY.
- Pšenčík, I. and Farra, V., 2005, First-order ray tracing for qP waves in inhomogeneous weakly anisotropic media, *Geophysics*, 70, D65-D75.
- Schoenberg, M. and Helbig, K., 1996. Orthorhombic media: Modeling elastic wave behavior in a vertically fractured earth: *Geophysics*, 62, 1954-1974.
- Shearer, P.M., 1999, *Introduction to seismology*, Cambridge University Press, Cambridge, UK.
- Tsvankin, I., 2001, *Seismic signatures and analysis of reflection data in anisotropic median*, Pergamon Press, Elsevier Science Ltd., Amsterdam.
- Tang, W. and Li, L., 2008, Exact travelttime computation in multi-layered transversely isotropic media with vertical symmetry axis, *Acta Seismologica Sinica*, 21(4), 370,379.
- Zhou, B. and Greenhalgh, S.A., 2004, Raypath and travelttime computations for 2D transversely isotropic media having dipping symmetry axes, *Exploration Geophysics*, 37, 150-159.

Model	A₁₁	A₃₃	A₅₅	A₁₃	ε	σ
Olivine	15.06	10.84	3.12	1.64	0.179	-0.415

Table 1. The transversely isotropic model used in the figures. The A_{ij} have the dimensions of (velocity)² and the two dimensionless parameters, ϵ and σ , are indicators of the degree of anisotropy. The quantity $\epsilon = \sqrt{A_{11}/A_{33}} - 1$ is a measure of the ellipticity of the qP wavefront, while $\sigma = A_D / [2A_{33}(A_{33} - A_{55})]$ defines the deviation from the elliptical (spherical) for the qP (qS_V) wavefronts or equivalently, slowness surfaces. $(A_D = (A_{13} + A_{55})^2 - (A_{11} - A_{55})(A_{33} - A_{55}) = -69.5192)$. $A_D(E_{13}) = \sigma = 0$, corresponds to the elliptical (spherical) case. In the linearized formulation, $\sigma = E_{13} / 2\sqrt{A_{11}A_{33}} = -0.397$ ($E_{13} = -10.14$).

ACKNOWLEDGEMENTS

The support of the sponsors of CREWES is duly noted. The first author also receives assistance from NSERC through operating and strategic grants held by Professors E.S. Krebs, L.R. Lines and G. F. Margrave.

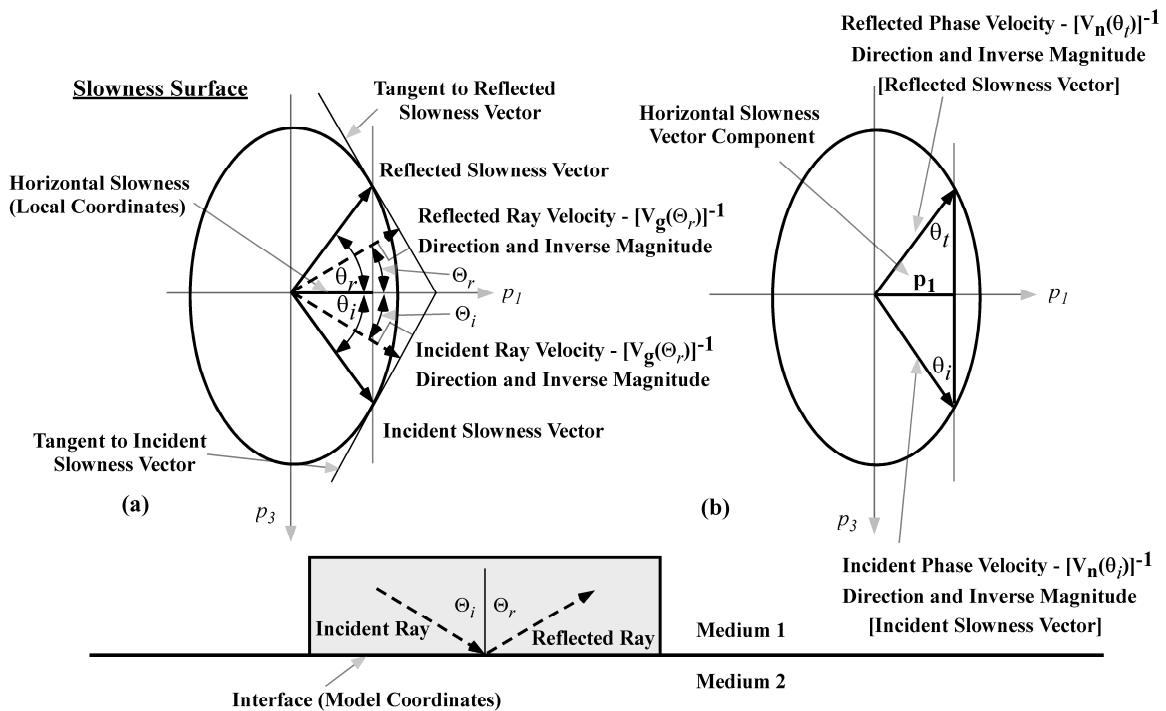


FIG. 1. The simple reflection of a qP ray due to incidence from a TI medium on a plane interface. There is no rotation of the anisotropic axis with respect to the model coordinates. Part (a) indicates the relationship in slowness space between magnitudes of the inverse of the phase velocity (slowness) vector and the inverse of the group velocity vector. Their directions are the same in Cartesian spatial coordinates as in slowness space. The determination of the reflected phase angle, θ_r , in terms of the tangential component of the slowness vector, p_1 , is given in part (b). It may be seen that all which is required for the (generally numerical) computation of this quantity is the application of basic analytic geometry, involving right angled triangles. In the shaded region are shown the directions of the incident and reflected ray (group) vectors. The lengths of these vectors are inversely proportional to their magnitudes in Cartesian ray space.

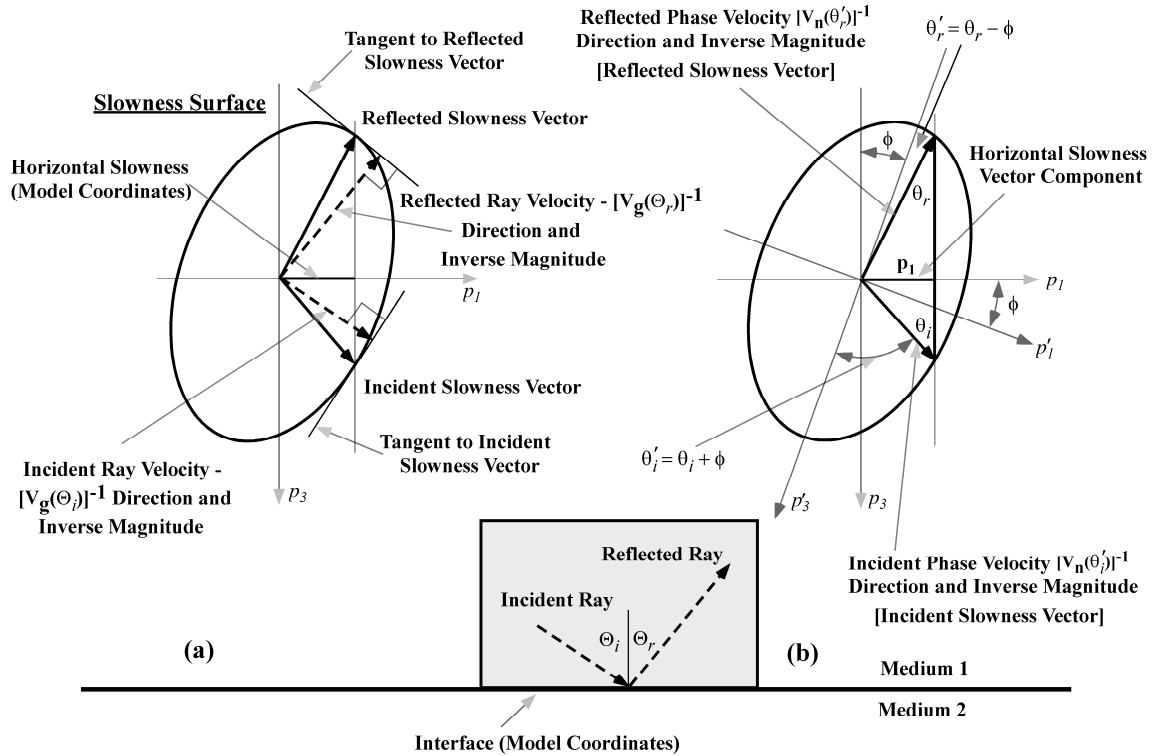


FIG. 2. A more complicated reflection of a qP ray due to incidence from a TI medium on a plane interface. In this case there is rotation of the anisotropic axis by the angle ϕ (measured positive clockwise) with respect to the model coordinates. As in Figure 1, part (a) shows how the inverse magnitude of the phase velocity (slowness) vector and the inverse magnitude of the group velocity vector are related. Part (b) displays the manner in which the reflected phase angle, θ_r , is obtained in terms of the tangential component of the slowness vector, p_1 , in a marginally more complex manner than in Figure 1. However, as in the previous example, only basic analytical geometric relationships are required to formulate the solution method in a numerically solvable equation. In the shaded region are shown the directions of the incident and reflected ray (group) vectors. The lengths of these vectors are inversely proportional to their magnitudes in Cartesian ray space.

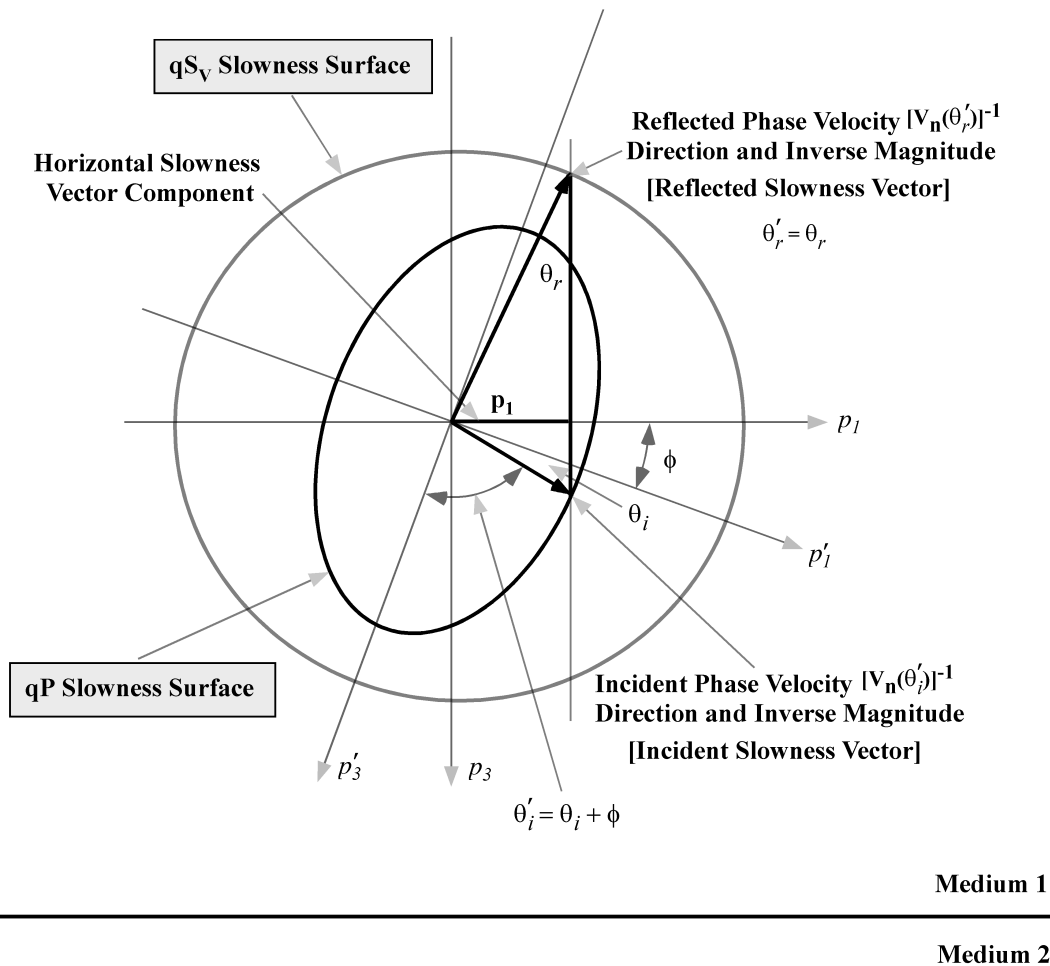


FIG. 3. The analogue of Snell's Law for a qP wave incident on a plane interface with a reflected qS_V wave resulting. The qP slowness surface is rotated by an angle qP with respect to the interface and as it has been indicated to be elliptical, the qS_V slowness surface is forced to be circular. This degenerate case is the exception rather than the norm for TI media. As the qS_V slowness surface is circular, the reflected slowness vector will have the same magnitude at any angle, hence $(\theta'_r = \theta_r)$. It is necessary, however, to determine the angle θ_r to fully specify the reflected qS_V slowness vector, given that p_1 is assumed known.

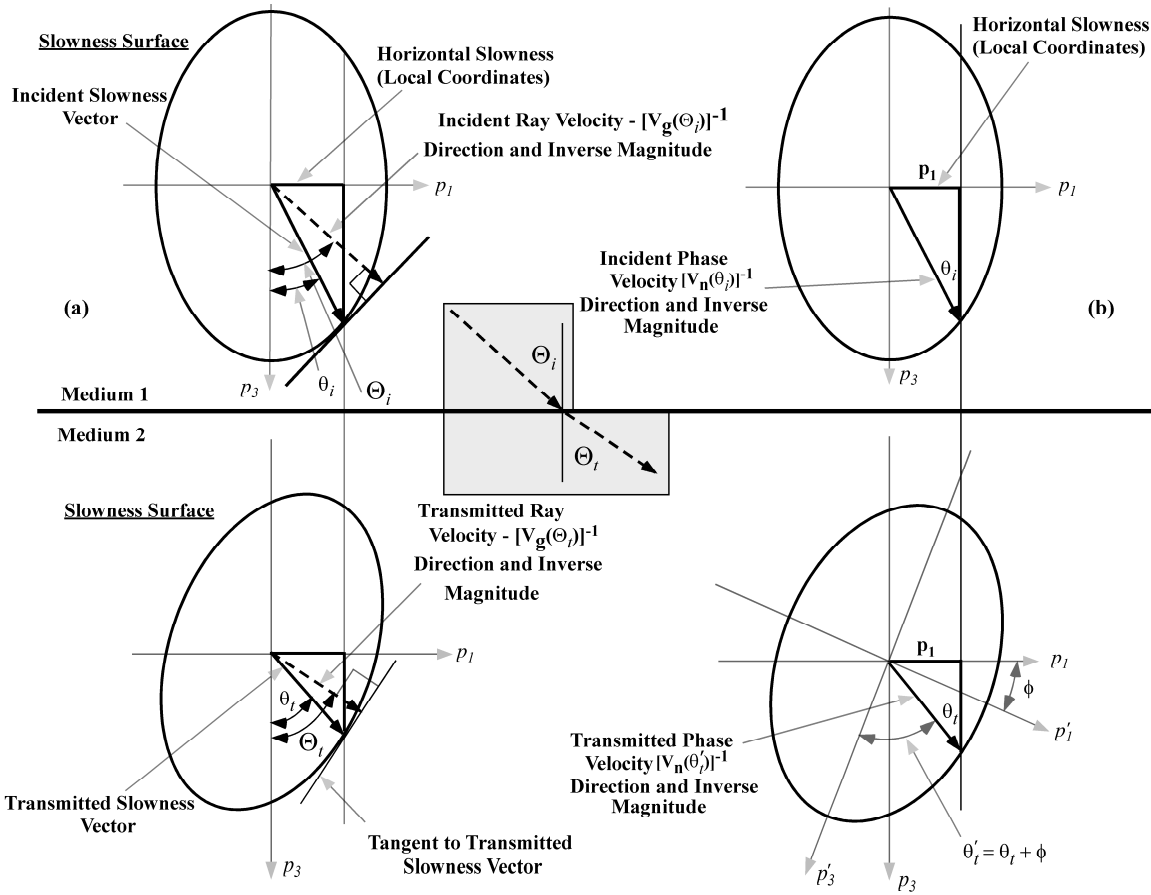


FIG. 4. A transmitted qP ray in medium 2, a TI medium, due to incidence from medium 1, also a TI medium, on a plane interface separating the two media. There is rotation of the anisotropic axis in medium 2 by the angle ϕ (measured positive clockwise) with respect to the model coordinates. Again, part (a) shows how the inverse magnitude and direction of the phase velocity (slowness) vector and the inverse magnitude and direction of the group velocity vector are related. In a manner similar to Figure 2, part (b) depicts the manner in which the transmitted phase angle, θ_t , is obtained in terms of the tangential component of the slowness vector, p_1 . As in Figures 1 and 2, only uncomplicated analytical geometric formulae are needed to construct the numerically solvable solution. As in previous figures, in the shaded region are shown the directions of the incident and reflected ray (group) vectors. The lengths of these vectors are inversely proportional to their magnitudes in Cartesian ray space.

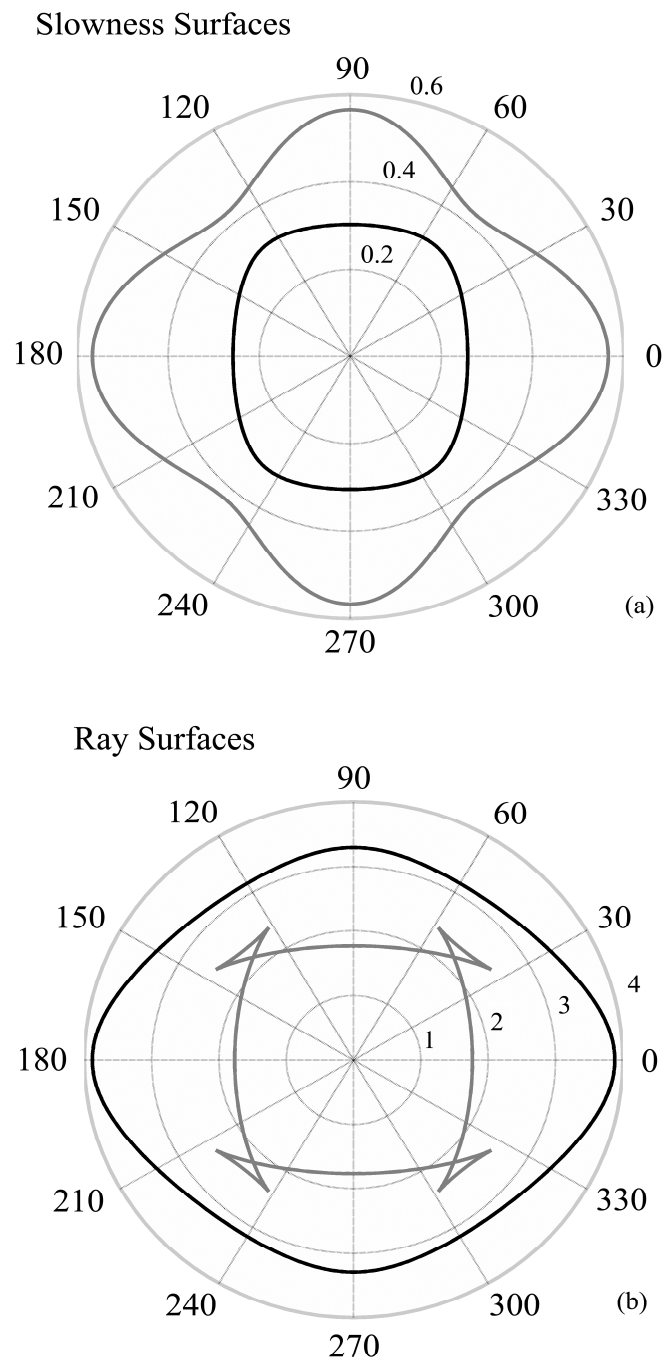


FIG. 5. The qP (black) and qS_V (gray) slowness surfaces for a symmetry section of olivine are shown in polar form in panel (a). The dimensions are in s/km and the computations are done using the parameters given in Table 1. Panel (b) shows the ray surfaces for these two propagation modes also plotted in polar notation again with qP (black) and qS_V (gray). The dimensions are in km/s .

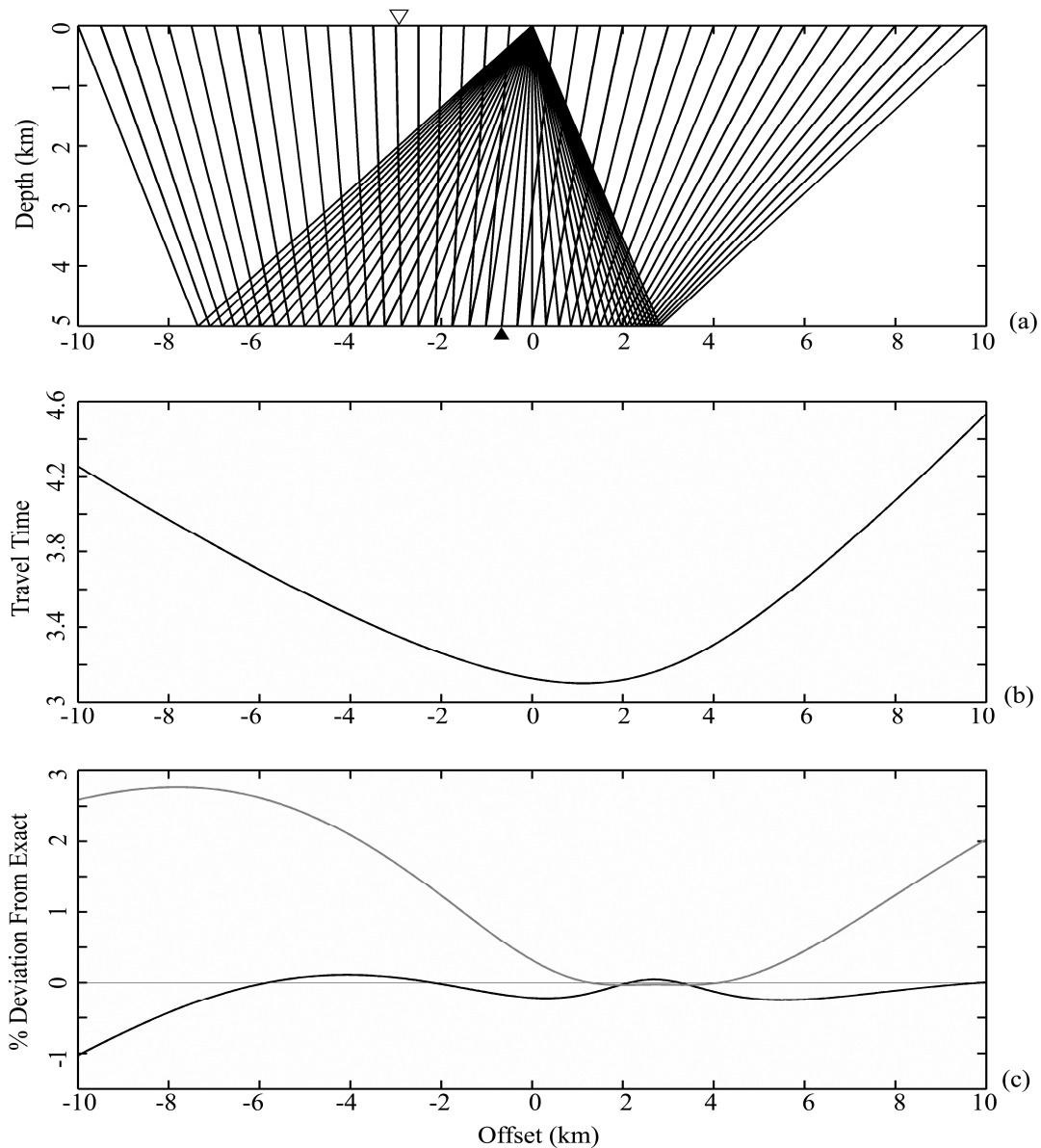


FIG. 6. Two point ray tracing with a qP ray incident and qP ray reflected from the plane interface at a depth of 5km . The ray paths drawn at 0.5km intervals for surface receivers located at offsets of -10km to 10km are shown in panel (a). The exact method discussed in the text was used for this with the anisotropic axis rotated 15° with respect to model coordinates. The solid triangle in (a) indicates the point where the reflected ray returns to the source, and the open triangle the ray which is at normal incidence at the surface. The exact travel time for this reflected qP ray is shown in panel (b), while the differences in travel times in percent of the approximate method (gray) and linearized method (black) when compared to the exact method are plotted in panel (c).

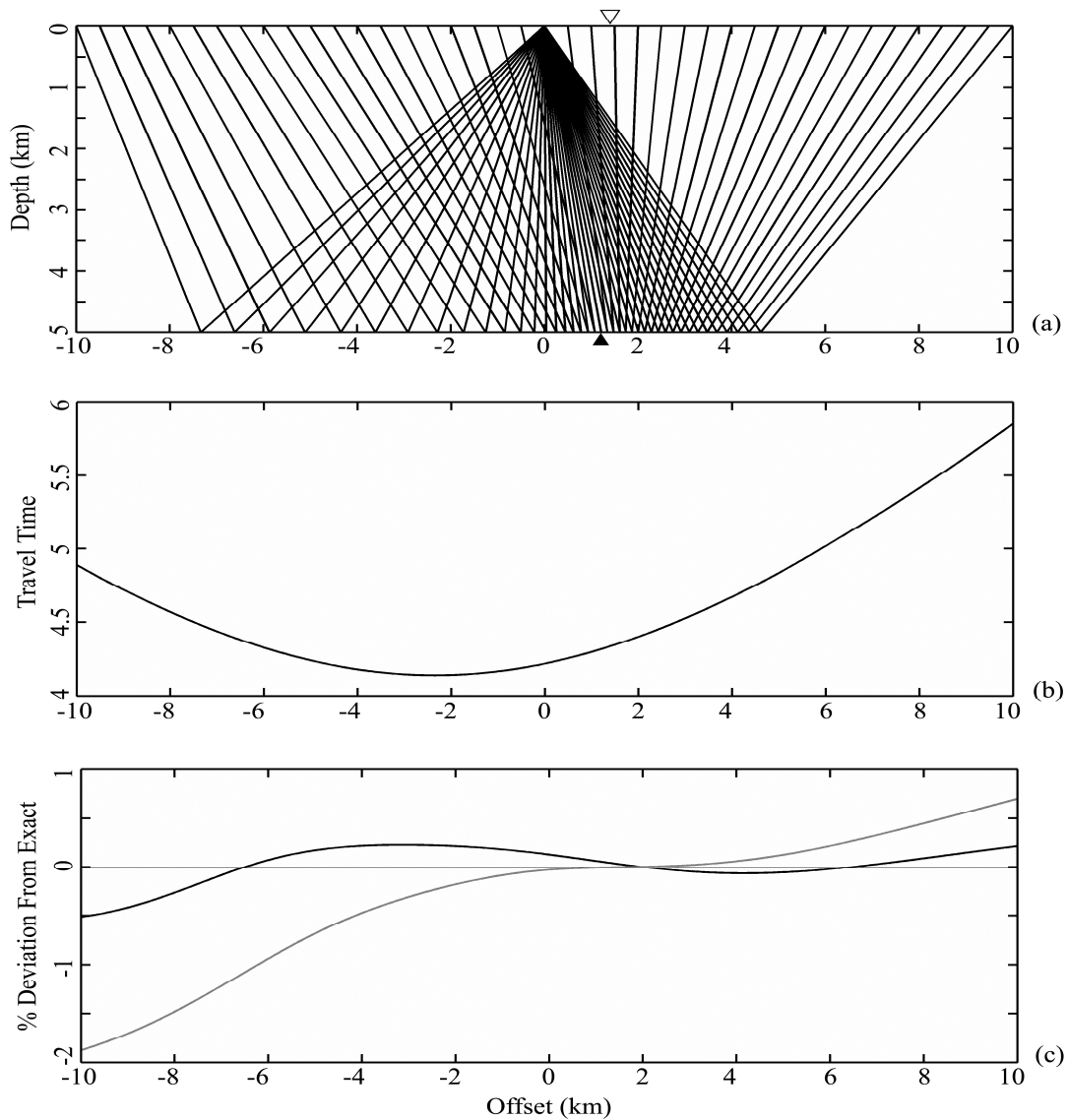


FIG. 7. Two point ray tracing with a qP ray incident and a qS_V ray reflected from the plane interface at a depth of 5 km . The ray paths drawn at 0.5 km intervals for surface receivers located at offsets of -10 km to 10 km are shown in panel (a). The exact method discussed in the text was used for this with the anisotropic axis rotated 15° with respect to model coordinates. The solid triangle in (a) indicates the point where the reflected ray returns to the source, and the open triangle the ray which is at normal incidence at the surface. The exact travel time for this reflected $qP - qS_V$ ray is shown in panel (b), while the differences in travel times in percent of the approximate method (gray) and linearized method (black) when compared to the exact are plotted in panel (c).

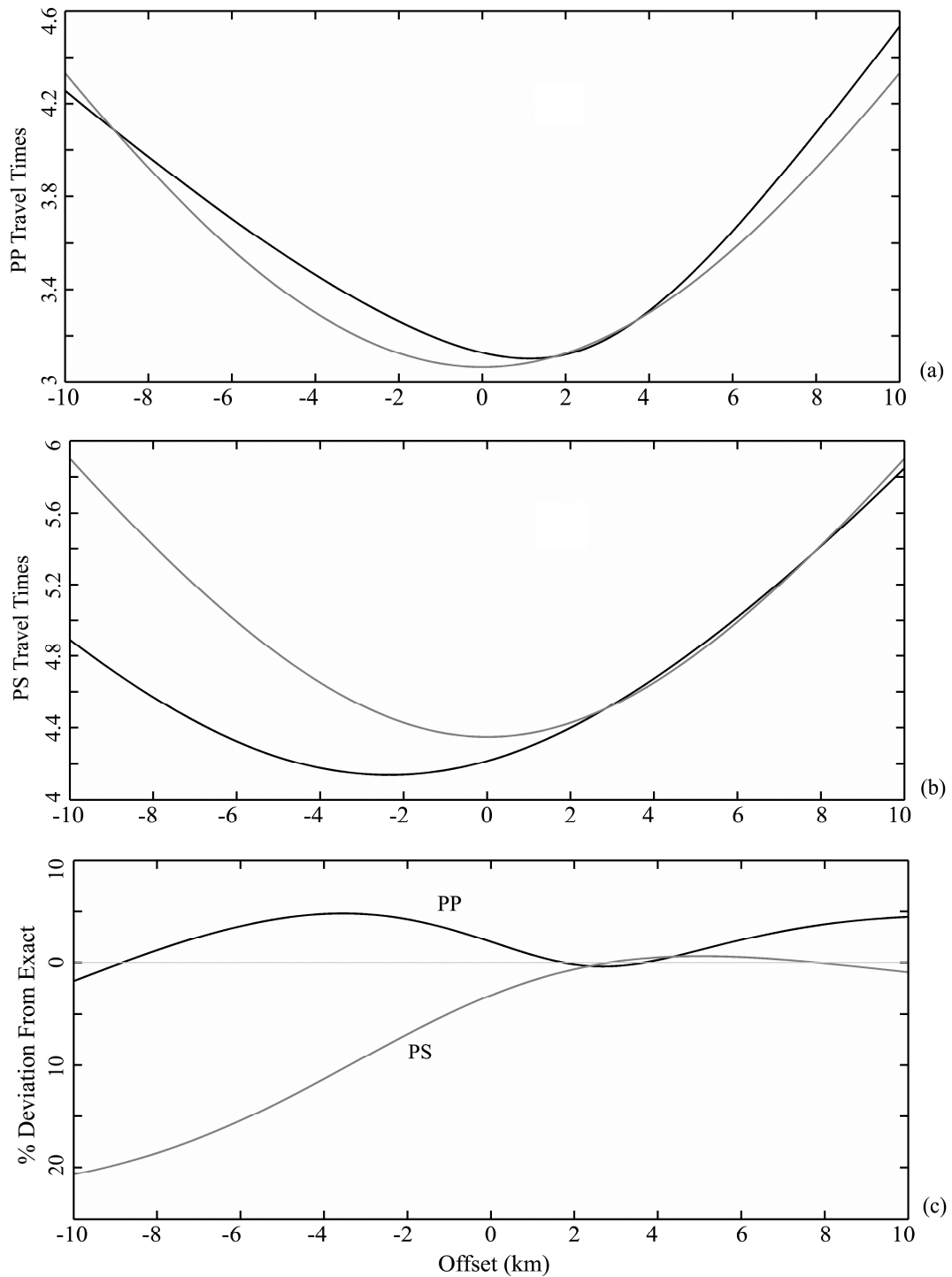


FIG. 8. Comparisons of travel times for the reflected (a) PP and (b) PS rays for the exact anisotropic case (black) and the isotropic case (gray). The differences in percent are given in panel (c).